IAA-AAS-DyCoSS2-14 -01-03

# SELF-ORGANISING LOW EARTH ORBIT CONSTELLATIONS FOR EARTH OBSERVATION

**Garrie S. Mushet*** **and Colin R. McInnes†**

This paper presents a novel method of manipulating the spatial pattern of a fractionated micro-satellite constellation in Low Earth Orbit. The method developed allows satellites to manipulate the longitudinal position of their ground-tracks over the Earth's surface, such that they pass over specified targets. This is achieved firstly by pairing satellites on the constellation to the targets on the Earth's surface, and then by developing an artificial potential field controller to define the thrust commands which move the satellites into the appropriate orbital slots to converge upon their targets. The latter is achieved using Coupled Selection Equations - a dynamical systems approach to combinatorial optimisation.

## INTRODUCTION

To date, most satellite constellation applications have involved static constellations where satellites on common orbits maintain fixed relative positions, including Galileo, Globalstar, and the GPS constellations.[1,2,3] As a result, the key goal of traditional constellation design has been to minimise the number of satellites with respect to mission coverage requirements.[4,5]

However, recent developments in low-cost spacecraft technologies, miniaturisation and mass-production, are widening access to space, and are predicted to give rise to future deployments of much larger satellite constellations than those which have been traditionally implemented.[6,7] Such constellations offer many operational advantages over single-satellite platforms. For example, constellation reliability is increased, as the failure of a number of agents does not comrpomise the constellation as a whole. Additionally, since satellite demand is not uniformly distributed across the Earth's surface in most constellation applications, a self-organising micro-satellite constellation which allocates resources to match demand could offer a more efficient alternative to current constellations which provide static coverage irrespective of demand.

To enable such constellations, a new paradigm in satellite control must be realised, as the traditional approach of satellite constellation control, in which ground operators design and command station-keeping manoeuvres does not scale effectively to applications in which the number of spacecraft extends into the hundreds or even thousands. In addition, current operations only allow for small manoeuvres to maintain satellite positioning. For lower operational costs, faster response times, and improvements in the flexibility of the constellation, on-board autonomous control and decision-making protocols are likely.

There has been much work in the literature on the use of autonomous constellation control, but

*PhD Student, Dept. of Mechanical & Aerospace Engineering, University of Strathclyde, Glasgow, UK.
†Professor, Dept. of Mechanical & Aerospace Engineering, University of Strathclyde, Glasgow, UK.

this has mainly been for small station-keeping manoeuvres noted above, and not for complete reconfiguration of a small satellite constellation.[8,9,10,11,12,13,14]

This raises a unique set of engineering challenges. The use of resource-limited micro-satellites on such a constellation limits their individual operational capability. For best results, it is likely that the satellites could be fractionated - i.e. the constellation would consist of heterogeneous satellites with specific capabilities, which must collaborate to achieve mission goals. In addition, on-board computation must be performed across the many members of the constellation due to the limited computing performance of each agent, and results effectively communicated throughout the constellation. There is growing support in the literature for effective distributed/parallel computing capabilities amongst small satellite constellation members.[15,16,17]

This paper presents a novel solution to the problem of autonomous task allocation and reconfiguration / manoeuvring for a self-organising micro-satellite constellation in Low Earth Orbit. The method allows satellites, which are placed on Low Earth Orbits with repeat ground tracks, to shift their ground tracks such that they pass over targets on the Earth's surface to which they are assigned. This is achieved using Coupled Selection Equations - a dynamical systems approach to combinatorial optimisation whose solution tends asymptotically to a Boolean matrix describing the pairings of satellites and targets which solves the relevant assignment problem.[18] Satellite manoeuvres are actuated by low thrust propulsion, and thrust commands are generated by an artificial potential field controller which incorporates the Coupled Selection Equation output.

The remainder of this paper is organised as follows. The next section introduces the constellation model used, which consists of two polar low Earth orbital planes containing Earth imaging satellites, where the satellites on each image different wavelengths. The relevant dynamics associated with constellation ground tracks are investigated. In the section which follows, the task assignment problem relevant to the constellation design is introduced, and Coupled Selection Equations are introduced as a solution to the assignment problem. The artificial potential field controller is then derived in the penultimate technical section. Results from a demonstration simulation are then given and discussed. Finally, extensions of the method are discussed, and conclusions are given.

## CONSTELLATION DESIGN AND GROUND TRACK DYNAMICS

In this paper, a constellation is designed with two circular orbits inclined at an angle of $60^\circ$ to the equatorial plane, with the planes separated by right ascension of the ascending nodes, such that $\Delta\Omega = 180^\circ$.

The nominal semi-major axis, $a_{\text{nominal}}$, is set such that the satellites have a repeat groundtrack, with an orbital period set in a 16:1 ratio with the Earth's rotational period, i.e. $a_{\text{nominal}} = 6,640$ km.

On each orbit, $N$ satellite members are initially azimuthally equispaced, as described by Equation (1), and depicted in Figure 1.

$$\left.\begin{aligned} a_{i0} &= a_{\text{nominal}} \\ f_{i0} &= \frac{2\pi(i-1)}{N} \end{aligned}\right\} (i = 1, \ldots, N) \tag{1}$$

where $f$ is the true anomaly of the satellites.

In addition, the constellation will be fractioned such that the satellites on one orbit are of one *type*, and the satellites on the other are of another *type*. In this paper, an Earth observation mission

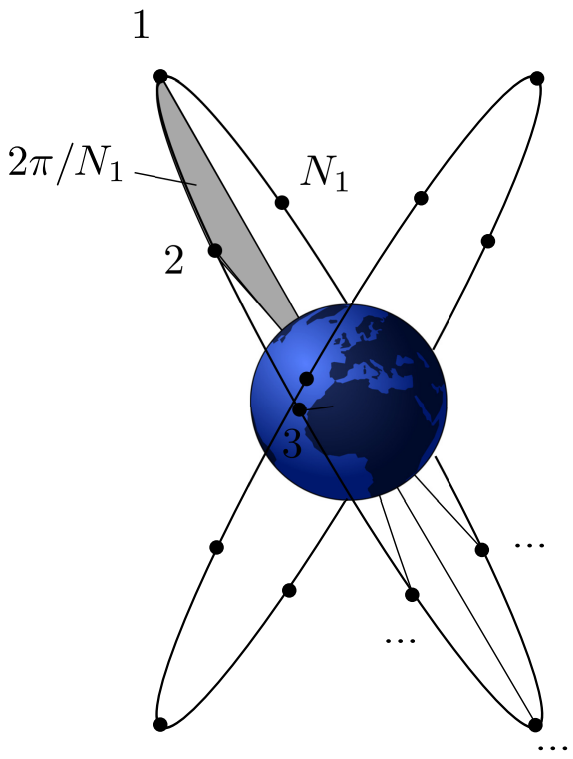


**Figure 1. Depiction of satellite constellation design.**

application is investigated in which, for example, the satellites on one orbit image at a specific wavelength, whilst the others image in a separate wavelength, enabling multi-spectral imaging.

The trajectories of each satellite are propagated according to the Gaussian form of the variation of Keplerian elements given in Equations (2)-(7).

$$\dot{a} = \frac{2a^2v}{\mu}a_t \tag{2}$$

$$\dot{e} = \frac{1}{v}\left[2\left(e+\cos\left(\theta\right)\right)a_t - \frac{r}{a}\sin\left(\theta\right)a_n\right] \tag{3}$$

$$\dot{i} = \frac{r\cos\left(u\right)}{h}a_h \tag{4}$$

$$\dot{\omega} = \frac{1}{ev}\left[2\sin\left(\theta\right)a_t + \left(2e+\frac{r}{a}\cos\left(\theta\right)\right)a_n\right] - \frac{r\sin\left(u\right)\cos\left(i\right)}{h\sin\left(i\right)}a_h \tag{5}$$

$$\dot{\Omega} = \frac{r\sin\left(u\right)}{h\sin\left(i\right)}a_h \tag{6}$$

$$\dot{M} = \sqrt{\frac{\mu}{a^3}} - \frac{b}{eav}\left[2\left(1+\frac{e^2r}{p}\right)\sin\left(\theta\right)a_t + \frac{r}{a}\cos\left(\theta\right)a_n\right] \tag{7}$$

where $a$ is the semi-major axis, $e$ is the eccentricity, $i$ is the inclination, $\omega$ is the argument of perigee, $\Omega$ is the right ascension of the ascending node, $M$ is the mean anomaly, $v$ is the orbital speed, $f$ is the true anomaly, $r$ is the orbital radius, $h$ is the specific angular momentum, $b$ is the semi-minor axis, $p$ is the semi-parameter, $\mu$ is the standard gravitational parameter of Earth, and $a_t$, $a_n$ and $a_h$

are the spacecraft accelerations in the directions tangential and normal to the velocity vector, and in the out-of-plane direction, respectively.

It is assumed that the spacecraft only have the ability to thrust in the tangential direction, that the satellite orbits remain quasi-circular throughout the low-thrust manoeuvres, and that there will be no out-of-plane motion. Orbit precession due to $J_2$ is ignored in this initial study.

Applying these assumptions, the equations of motion simplify to those given in Equations (8)-(13)

$$\dot{a} = 2\sqrt{\frac{a^3}{\mu}}a_t \tag{8}$$
$$\dot{e} = 0 \tag{9}$$
$$\dot{i} = 0 \tag{10}$$
$$\dot{\omega} = 0 \tag{11}$$
$$\dot{\Omega} = 0 \tag{12}$$
$$\dot{f} = \sqrt{\frac{\mu}{a^3}} \tag{13}$$

In order to enable tasking of each satellite, the orbit kinematics can be used to define the ground tracks. The position vector for a satellite on a circular orbit in the PQW reference frame, in which the origin lies at the Earth's centre, $\hat{\mathbf{P}}$ points to the orbit perigee, $\hat{\mathbf{Q}}$ points out of the orbit plane, and $\hat{\mathbf{Q}}$ completed a right-handed coordinate system, is given in Equation (14).

$$\mathbf{r}_{\text{PQW}} = [r\cos(f), r\sin(f), 0]^T \tag{14}$$

This can be transformed to the Earth Centred Earth Fixed (ECEF) reference frame, as shown in Figure 2 in which the origin again lies at the centre of the Earth, but with the $X$-axis pointing along the Greenwich meridian, the $X$-axis pointing to the North pole, and the $Y$-axis completing a right-handed coordinate system, via a series of matrix tranformations as given in Equation (15)*.

$$\mathbf{r}_{\text{ECEF}} = R_3(\theta)R_3(\omega)R_1(i)R_3(\Omega)\mathbf{r}_{\text{PQW}} \tag{15}$$

where $\theta$ is the Greenwich sidereal hour angle.

Taking the arbitrary choice of $\omega = 0$ for the circular orbits, this results in Equation (16).†

$$\mathbf{r}_{\text{ECEF}} = r\begin{pmatrix} \text{c}(f)\text{c}(\Omega)\text{c}(\theta) - \text{s}(f)\text{s}(\Omega)\text{c}(\theta) - \text{c}(f)\text{s}(\Omega)\text{c}(i)\text{s}(\theta) - \text{s}(f)\text{c}(\Omega)\text{c}(i)\text{s}(\theta) \\ \text{c}(f)\text{c}(\Omega)\text{s}(\theta) - \text{s}(f)\text{s}(\Omega)\text{s}(\theta) + \text{c}(f)\text{s}(\Omega)\text{c}(i)\text{c}(\theta) + \text{s}(f)\text{c}(\Omega)\text{c}(i)\text{c}(\theta) \\ \text{c}(f)\text{s}(\Omega)\text{s}(i) + \text{s}(f)\text{c}(\Omega)\text{s}(i) \end{pmatrix} \tag{16}$$

The elements of the position vector in the ECEF reference frame can be used to calculate the longitude, $\lambda$, and latitude, $\phi$, of the sub-satellite point, providing a trace of the satellite ground track over its orbit, as given by Equations (17)-(18).

$$\text{t}(\lambda) = \frac{r_y}{r_x} = \frac{\text{c}(f)\text{c}(\Omega)\text{s}(\theta) - \text{s}(f)\text{s}(\Omega)\text{s}(\theta) + \text{c}(f)\text{s}(\Omega)\text{c}(i)\text{c}(\theta) + \text{s}(f)\text{c}(\Omega)\text{c}(i)\text{c}(\theta)}{\text{c}(f)\text{c}(\Omega)\text{c}(\theta) - \text{s}(f)\text{s}(\Omega)\text{c}(\theta) - \text{c}(f)\text{s}(\Omega)\text{c}(i)\text{s}(\theta) - \text{s}(f)\text{c}(\Omega)\text{c}(i)\text{s}(\theta)} \tag{17}$$

*Rotation matrices given in Appendix.

†$\sin(\psi)$, $\cos(\psi)$ and $\tan(\psi)$ are shortened to $\text{s}(\psi)$, $\text{c}(\psi)$ and $\text{t}(\psi)$ from this point onwards due to some lengthy equations.

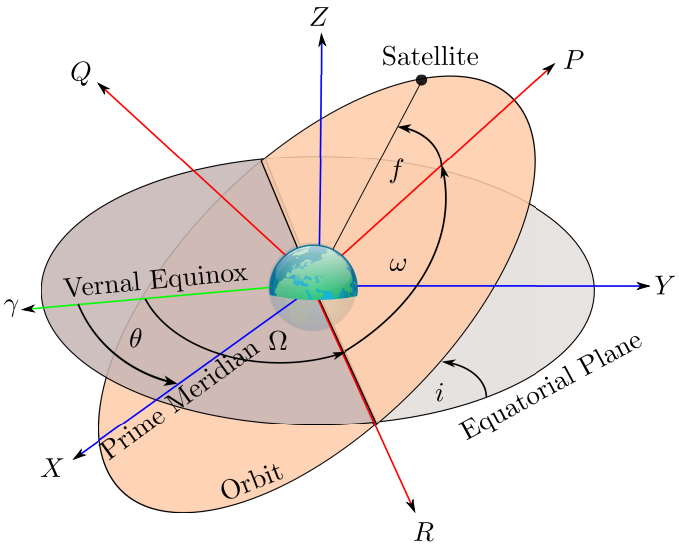


**Figure 2. Visualisation of the relationship between the $PQW$ reference frame, and the ECEF reference frame.**

$$\mathrm{s}(\phi) = \frac{r_z}{r} = \mathrm{s}(i)\mathrm{s}(f+\Omega) \tag{18}$$

Finally, since $\theta = \omega_{\oplus} t + \theta_0$, where $\omega_{\oplus}$ is the earth's rotational speed and $t$ is the time variable, and $f = \dot{f}t + f_0$, $\theta$ can be substituted for $\theta = \eta(f - f_0) + \theta_0$, where $\eta$ is the ratio of the satellite orbital period to the period of the Earth's rotation (in this paper $\eta = 1/16$), to make $f$ the only independent variable of the longitude and latitude equations as in Equations (19)-(20).

$$\begin{aligned}\mathrm{t}(\lambda) = \Big(&\mathrm{c}(f)\mathrm{c}(\Omega)\mathrm{s}(\eta(f-f_0)+\theta_0) - \mathrm{s}(f)\mathrm{s}(\Omega)\mathrm{s}(\eta(f-f_0)+\theta_0) + \\ &\mathrm{c}(f)\mathrm{s}(\Omega)\mathrm{c}(i)\mathrm{c}(\eta(f-f_0)+\theta_0) + \mathrm{s}(f)\mathrm{c}(\Omega)\mathrm{c}(i)\mathrm{c}(\eta(f-f_0)+\theta_0)\Big) / \\ &\Big(\mathrm{c}(f)\mathrm{c}(\Omega)\mathrm{c}(\eta(f-f_0)+\theta_0) - \mathrm{s}(f)\mathrm{s}(\Omega)\mathrm{c}(\eta(f-f_0)+\theta_0) - \\ &\mathrm{c}(f)\mathrm{s}(\Omega)\mathrm{c}(i)\mathrm{s}(\eta(f-f_0)+\theta_0) - \mathrm{s}(f)\mathrm{c}(\Omega)\mathrm{c}(i)\mathrm{s}(\eta(f-f_0)+\theta_0)\Big)\end{aligned} \tag{19}$$

$$\mathrm{s}(\phi) = \mathrm{s}(i)\mathrm{s}(f+\Omega) \tag{20}$$

In this paper, the aim is to shift the satellite ground tracks of assigned satellites in longitude, such that the ground track passes over specified targets. This is achieved by moving the satellite to different positions on its orbit. The arc of true anomaly by which the satellite must shift, $\Delta f$, is calculated using the equations for latitude and longitude.

Consider two satellites on the same circular orbit, but shifted in true anomaly, hence $\Omega_1 = \Omega_2 = \Omega$, $i_1 = i_2 = i$, and $f_1 = f_2 - \Delta f$. Now, if we consider the latitude equation for the second satellite at time $t = t_0 = 0$, and assuming that $\theta_0 = 0$, it can be shown that:

$$\mathrm{t}(\lambda_2(0)) = \mathrm{c}(i)\left(\frac{\mathrm{s}(\Omega)\mathrm{c}(\Delta f) + \mathrm{c}(\Omega)\mathrm{s}(\Delta f)}{\mathrm{c}(\Omega)\mathrm{c}(\Delta f) - \mathrm{s}(\Omega)\mathrm{s}(\Delta f)}\right) \tag{21}$$

Now, we consider the first satellite at a time $t = t_0 + \Delta t = \frac{\Delta f}{\dot{f}}$, i.e. after the satellite has traversed $\Delta f$ to arrive at the same latitude where satellite 2 was at $t = 0$, it can be shown that the longitude of satellite 1 is given by:

$$\begin{aligned}\mathrm{t}\left(\lambda_1(\Delta t)\right) = \Big(&\mathrm{c}(\Omega)\mathrm{c}\left(\Delta f\right)\mathrm{s}\left(\eta\Delta f\right) - \mathrm{s}(\Omega)\mathrm{s}\left(\Delta f\right)\mathrm{s}\left(\eta\Delta f\right) + \\ &\mathrm{s}(\Omega)\mathrm{c}(i)\mathrm{c}\left(\Delta f\right)\mathrm{c}\left(\eta\Delta f\right) + \mathrm{c}(\Omega)\mathrm{c}(i)\mathrm{s}\left(\Delta f\right)\mathrm{c}\left(\eta\Delta f\right)\Big)/ \\ &\Big(\mathrm{c}(\Omega)\mathrm{c}\left(\Delta f\right)\mathrm{c}\left(\eta\Delta f\right) - \mathrm{s}(\Omega)\mathrm{s}\left(\Delta f\right)\mathrm{c}\left(\eta\Delta f\right) - \\ &\mathrm{s}(\Omega)\mathrm{c}(i)\mathrm{c}\left(\Delta f\right)\mathrm{s}\left(\eta\Delta f\right) - \mathrm{c}(i)\mathrm{c}(\Omega)\mathrm{s}\left(\Delta f\right)\mathrm{s}\left(\eta\Delta f\right)\Big) \end{aligned} \quad (22)$$

The longitudinal shift, $\Delta\lambda$, is then given by subtracting the arctangent of Equation (22) from the arctangent of Equation (21), as given in Equation (23).

$$\Delta\lambda = \lambda_2(0) - \lambda_1(\Delta t) \quad (23)$$

By applying the trigonometric identities in Equations (24)-(26), it can be shown that Equation (23) simplfies to Equation (27).

$$\mathrm{s}(\eta\Delta f) = \sum_{k=0}^{\eta}\binom{\eta}{k}\mathrm{c}^k(\Delta f)\mathrm{s}^{\eta-k}(\Delta f)\mathrm{s}\left(\frac{1}{2}(\eta-k)\pi\right) \quad (24)$$

$$\mathrm{c}(\eta\Delta f) = \sum_{k=0}^{\eta}\binom{\eta}{k}\mathrm{c}^k(\Delta f)\mathrm{s}^{\eta-k}(\Delta f)\mathrm{c}\left(\frac{1}{2}(\eta-k)\pi\right) \quad (25)$$

$$\mathrm{t}^{-1}(\alpha) - \mathrm{t}^{-1}(\beta) = \mathrm{t}^{-1}\left(\frac{\alpha-\beta}{1+\alpha\beta}\right) \quad (26)$$

So that

$$\Delta\lambda = -\eta\Delta f \quad (27)$$

Hence, the shift in longitude of the ground track is dependent only on the change in orbital position, and the ratio of the orbital period to the period of Earth's rotation. For example, for a period ratio of 16, a $10^\circ$ Westward longitudinal shift requires the satellite to move to an orbital slot $160^\circ$ ahead of its nominal position.

The required $\Delta\lambda$ for any satellite to converge upon a target of known latitude and longitude to which it is assigned is calculated using Equations (19)-(20). First Equation (20) is solved for $f$ given $\phi = \phi_{\text{target}}$. Solutions in $f$ are then passed to Equation (19) to calculate the satellite longitudes, $\lambda_{\text{satellite}}$, at those positions. The required longitudinal shifts for each $f$ solution is then calculated according to Equation (28).

$$\Delta\lambda = \lambda_{\text{satellite}} - \lambda_{\text{target}} \quad (28)$$

The smallest $\Delta\lambda$ is found, and passed to Equation (27) to calculate the required shift in orbital position, $\Delta f$, which is actuated using the artificial potential field controller described later in the paper.

The problem of assigning satellites to targets will now be considered.

## TASK ASSIGNMENT AND COUPLED SELECTION EQUATIONS

The problem of task allocation can be stated, in the context of this paper, as the problem of assignment pairs of satellites to targets on the Earth's surface, subject to some constraint.

In the case of a fractionated/disaggregated satellite constellation, where multiple *types* of satellite must be allocated to each target, this problem statement is best modelled mathematically by the axial three-index assignment problem.[18,19] For a constellation of two orbital planes and $N_{tgt}$ targets on the Earth's surface, where the number of satellites on the first and second plane are given by $N_{\text{sat1}}$ and $N_{\text{sat2}}$ respectively, this is stated as accordng to Eqs. (29) - (32).

$$\underset{c}{\text{minimise}} \qquad c = \sum_{i,j,k} C_{ijk} X_{ijk} \tag{29}$$

$$\text{subject to} \qquad \sum_{i} X_{ijk} = 1, \quad \forall (j,k) \in N_{\text{tgt}} \times N_1 \tag{30}$$

$$\sum_{j} X_{ijk} = 1, \quad \forall (i,k) \in N_{\text{tgt}} \times N_2 \tag{31}$$

$$\sum_{k} X_{ijk} = 1, \quad \forall (i,j) \in N_1 \times N_2 \tag{32}$$

Here, $N_1$, $N_2$, and $N_{\text{tgt}}$ are the numbers of satellites of type 1 (on orbit 1), type 2 (on orbit 2) and of targets, respectively. Then $c$ is the total cost of the assignments made, $C_{ijk}$ is the cost associated with pairing satellites $j$ and $k$ to target $i$, and $X_{ijk}$ is the Boolean variable which describes whether or not the assignment is to be made, as according to Eq. (33).

$$X_{ijk} = \begin{cases} 1 & \text{if satellites } j \text{ \& } k \text{ are to visit target } i \\ 0 & \text{otherwise} \end{cases} \tag{33}$$

The constraints described by Equations (30)-(32) represent the requirement that each pair of satellites can only be assigned to one target, and each target can only be assigned to one pair of satellites. As a result, $\mathbf{X} = [X_{ijk}]$ is a permutation matrix. In most micro-satellite applications, and in the mission scenario considered in this paper, it is desirable that multiple pairs of satellites be assigned to each target to increase the quality of service delivered by the constellation. To achieve this, targets are represented multiple times within the assignment problem depending on the number of imagers required.

Coupled Selection Equations are proposed as an elegant and efficient method of solving this assignment problem.[18] A selection equation is a dynamical system in which the modes of the system are matched against one another in a competition in which only one mode will win, while all other modes vanish, as depicted an example time evolution of the one-dimensional Coupled Selection Equation shown in Fig. 3, where $\xi$ represents the coupled selection variables, in this case for $i = 1, 2, ...5$.

In such a one-dimensional case, and in the most basic problems, this behaviour may seem trivial. However, in more complex situations and in higher dimensions, the coupled selection equations provide efficient solutions in the presence of complex interactions between the modes.

Additionally, coupled selection equations can be described as gradient flows with asymptotically stable equilibria. As a result, a simple first order Euler method integrator is sufficient for numerically propagating the equations, and convergence is usually reached within just a few hundred time

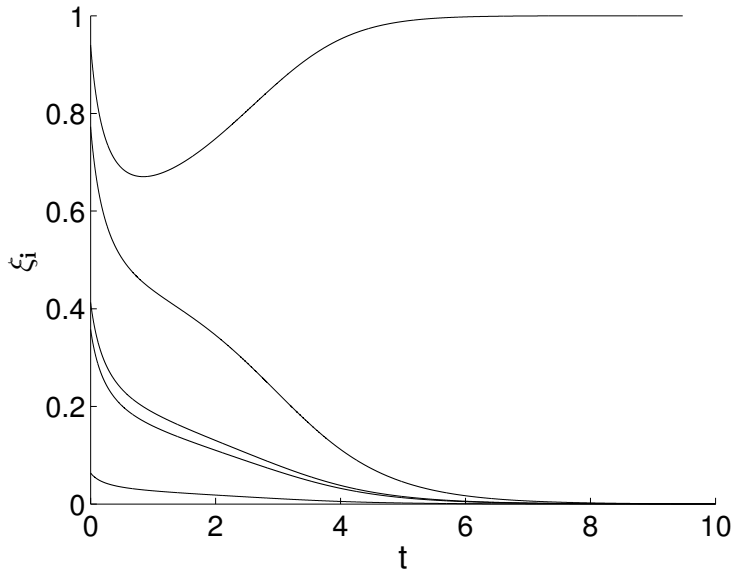


**Figure 3. Typical time evolution of coupled selection equations for 5 competing modes,** $i = 1, 2, ..., 5$**.**

steps. This is beneficial for implementation on a fractionated micro-satellite constellation, as the computing demand on the constellation would not be significant.

Due to the tendency for the highest initial values to persist in the coupled selection equation evolution, the assignment problem must be transformed to a maximisation problem rather than a minimisation problem. This is achieved simply by applying a linear transform to the costs to convert them to winnings, which are equivalent quantities to be maximised, as described in Equation (34).

$$W_{ijk} = -\gamma C_{ijk} + \delta, \quad \gamma > 0, \quad \gamma, \delta \in \mathbb{R} \forall (i, j, k) \in N_{\text{tgt}} \times N_{\text{sat1}} \times N_{\text{sat2}} \tag{34}$$

In this particular case, the three-index Coupled Selection Equation is best suited to solve the axial three-index assignment problem. This equation is given in Eq. (35).

$$\dot{\xi}_{ijk} = \xi_{ijk} \left( 1 + (3\beta - 1)\, \xi_{ijk}^2 - \beta \left( \sum_{i'} \xi_{i'jk}^2 + \sum_{j'} \xi_{ij'k}^2 + \sum_{k'} \xi_{ijk'}^2 \right) \right) \tag{35}$$

where $\xi_{ijk}$ is the coupled selection variable describing the strength of the connection between target $i$ and satellites $j$ and $k$.

The coupled selection variables are initialised with the winnings associated with each possible pairing, and their converged solution after integration provides the Boolean matrix which solves the assignment problem. The coupled selection equations restrict the values of $\xi_{ijk}$ to the interval [0,1]. Hence, in the linear transformation described in Equation (34), $\gamma = (\max(\mathbf{C}))^{-1}$ and $\delta = 1$ so as to normalise the initial coupled selection variables to the required range.

An example of the evolution of the three-index coupled selection equation is shown in Fig. 4, in a case where 3 satellites of type 1 and 3 satellites of type 2 must be allocated to 3 targets on the Earth's surface.

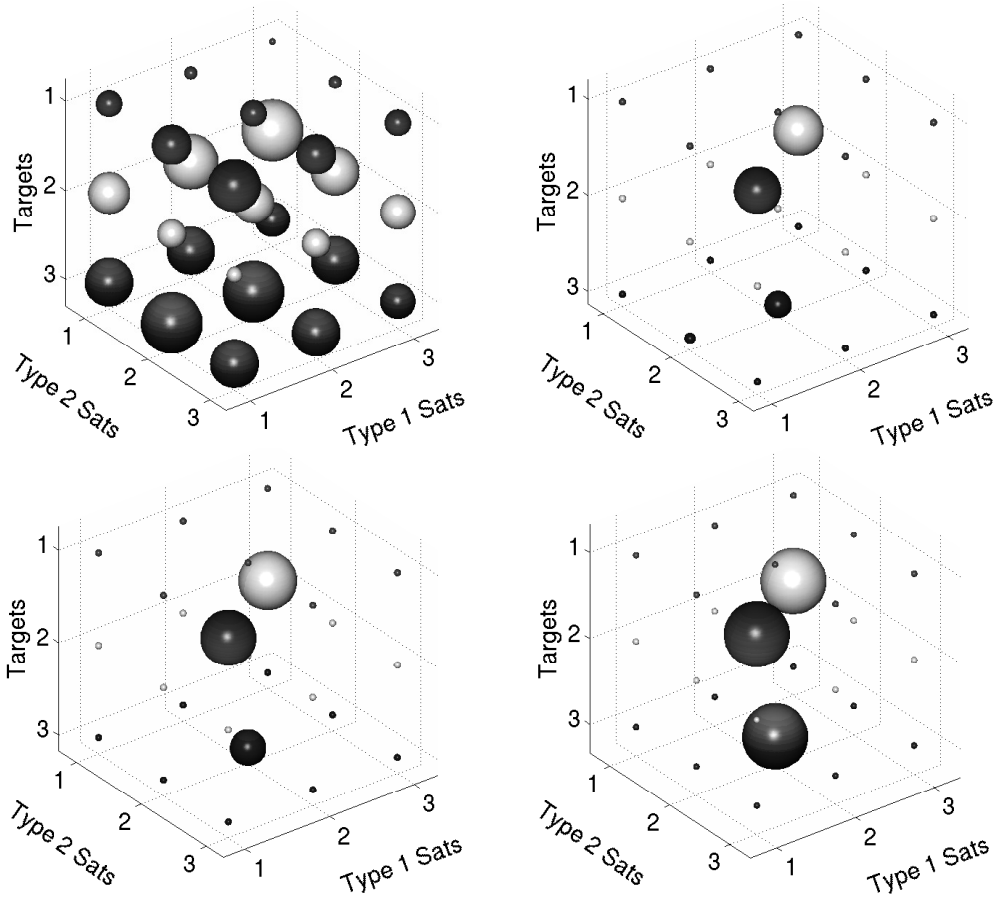


**Figure 4. Time evolutions of coupled selection equation variables - the radius of each sphere represents strength of pairing between the associated targets and satellites. Top left after 0 time steps, top right after 40 time steps, bottom left after 90 time steps, and bottom right after 140 time steps.**

Here, the top 3x3 layer represents the possible combinations of satellites from each type which can visit the first target, the middle 3x3 layer represents the possible combinations which can visit the second target, etc. The figure shows the convergence of the equations, which takes just a few seconds of computation. In the final converged state, only one sphere remains in each layer, indicating that the appropriate pairs to be allocated to each target has been decided. The time evolutions of these 9 coupled selection variables take just 140 time steps to converge, with the time steps needing for convergence scaling well with the number of agents available to perform computations.

In this work, the cost is defined as the sum of the phase angles which the satellite in each pair must traverse to align their ground tracks with the target, as described in Equation (36).

$$C_{ijk} = \Delta f_{ij} + \Delta f_{ik} \tag{36}$$

This definition has been chosen as the phase angle is proportional to the time taken for convergence in the minimum-time target visition problem, and also is proportional to the fuel expended in the minimum-fuel target visitation problem.

## ARTIFICIAL POTENTIAL FIELD CONTROLLER

Once the satellites have been allocated to targets by the converged solution of the coupled selection equations, low-thrust commands are generated by an artificial potential field controller which incorporates the coupled selection equation output.

In this paper a thrust-coast-thrust profile is adopted, in which the satellites traverse the required phasing angles by raising or lowering their orbit semi-major axis by a fixed offset, $a_{\text{offset}}$, with respect to the nominal semi-major axis for the repeat ground track orbit. The satellites then return to the nominal orbital radius once they have reached the target orbital slot. This is characterised by Equation (37).

$$a_{\text{desired}} = \begin{cases} a_{\text{nominal}} - a_{\text{offset}}\epsilon & |\Delta f| > |\Delta f_{\text{return}}| \\ a_{\text{nominal}} & |\Delta f| \leqslant |\Delta f_{\text{return}}| \end{cases} \tag{37}$$

where $\epsilon$ is a variable which is 1 when the satellite lags its target, and must lower the orbit to traverse the phase angle, or -1 when the satellite leads the target, and must raise the orbit, and $\Delta f_{\text{return}}$ is the phase angle through which the satellite would traverse as it thrusted towards the $a_{\text{nominal}}$. This is calculated analytically at each time step.

The artificial potential field is designed accoording to Equation 38.

$$V = \frac{1}{2} \sum_{j=1}^{N_1 \times N_2} \left(a_j - a_{\text{desired}}\right)^2 \tag{38}$$

where $a_{\text{desired}}$ is switched between the nominal orbit, and an offset from this nominal orbit depending on whether the satellite has arrived at the a target, or must drift towards it.

As a result of the parabolic shape of the potential function, convergence can be assured as long as the rate of change of the potential function is always negative.

The derivative of Eq. 38 is given by Eq. 39.

$$\dot{V} = \sum_{j=1}^{N_1 \times N_2} \dot{a}_j \left(a_j - a_{\text{desired}}\right) \tag{39}$$

Substituting the simplified satellite dynamics, a control law can be derived to ensure the derivative is always negative, as given in Eq. 40.

$$a_{tj} = -\zeta \text{sgn}\left(a_j - a_{\text{desired}}\right) \tag{40}$$

where $\zeta$ is a parameter describing the maximum acceleration magnitude available to the satellite. The value of $\zeta$ was set to 0.1 mm/s$^2$, equivalent to a 100 kg spacecraft with $10^{-2}$ N of available thrust, with $a_{\text{offset}} = 15$ km.

## MISSION SCENARIO SIMULATION

In this mission scenario simulation, 10 satellites were placed on the constellation, 5 on each of the orbits described in previous sections, initially equally spaced in true anomaly around orbits. A

**Table 1. Simulation Scenario Details**

| Target | Target Longitude [deg] | Target Positions (lat,long) (deg) | No. Of Satellites Per Target |
|---|---|---|---|
| 1 | 126 | 33.8 | 2 |
| 2 | -875 | 12.6 | 3 |

target scenario was simulated in which two targets appear on the Earth's surface, each demanding 2 and 3 pairs of satellites respectively, as detailed in Table 1.

Figure 5 shows the satellite ground tracks before any manoeuvring has taken place. It can be seen that the ground track coverage is uniform across the Earth's surface. However, although coverage is generally comprehensive, the quality of service available at any given location is poor due to the limited capabilities of individual satellites.

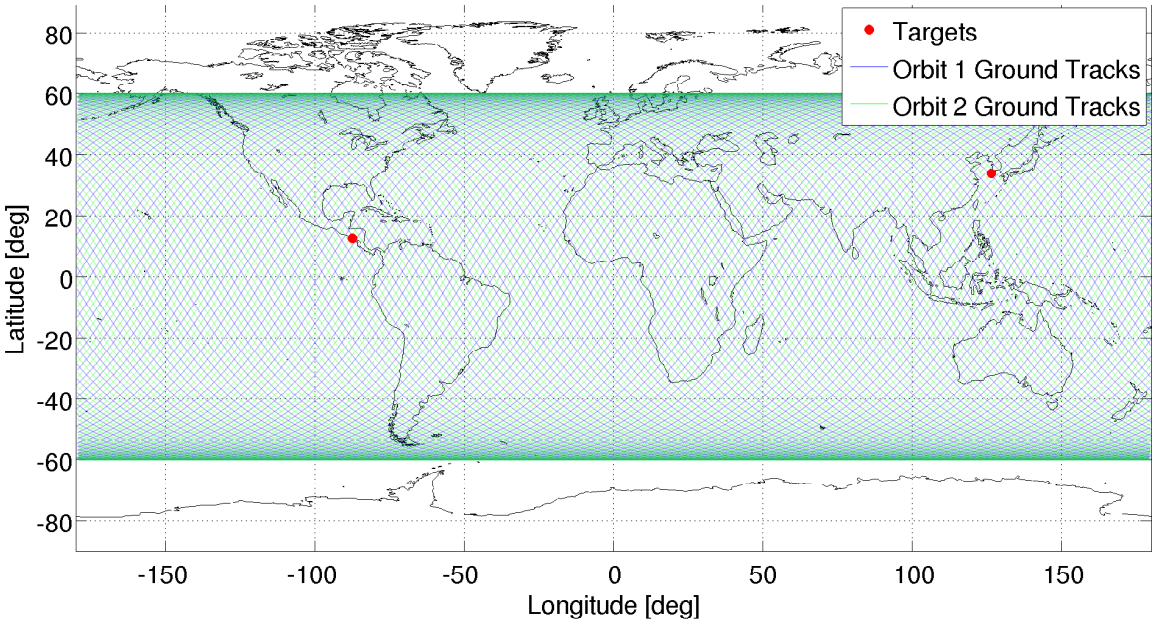


**Figure 5. Satellite repeat ground tracks for 1 Earth rotation before manoeuvring at $t = 0$ days. General coverage is good, but with low capabilities in each satellite, the quality of service at any location is low.**

Figure 6 displays the time history of the 125 Coupled Selection variables. The behaviour shown here indicates the complex interactions involved in the numerical propagation of the Coupled Selection Equations. In the first 100 integration steps, the majority of the variables vanish to zero, losing the competition. Others converge to one of two values constituting an unstable equilibrium of the system. Noise is added to the system at this stage to encourage convergence to stable equilibria, and at that point, the remaining variable compete, with the final 5 reaching convergence after close to 600 time steps.

In addition, the computational simplicity of the method is indicated by how few time steps are required for convergence. This increases as the number of targets, satellites and orbits (and hence

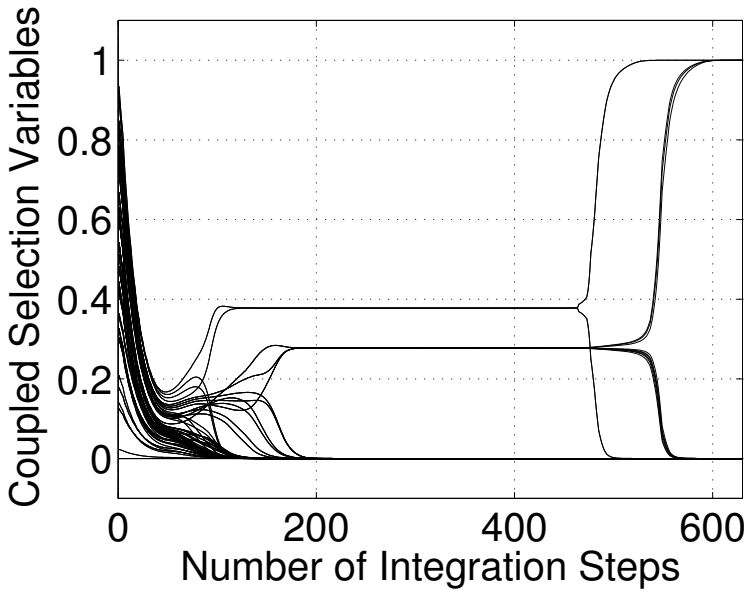


**Figure 6. Time histories of coupled selection variables, indicating the complex interactions involved in the convergence of complicated multi-dimensional constellations.**

dimension of the Coupled Selection Equation) increase, but not to unmanagable timescales and, depending on the processing availability distributed throughout the constellation, will only required computation times on the order of minutes.

After the coupled selection equations have converged satellites have been assigned to the targets in pairs, and initiate the thrust-coast-thrust phasing manoeuvres defined in the previous section. In this scenario, it takes 5.5 days of manoeuvring and an average $\delta v$ expenditure per satellite member of 0.027 $\mathrm{ms}^{-1}$ before the ground tracks are shifted above their respective targets, as shown in Figure 7. In addition, the time histories of satellite phase angles with respect to the orbital slots to which they were assigned are showin Figure 8.

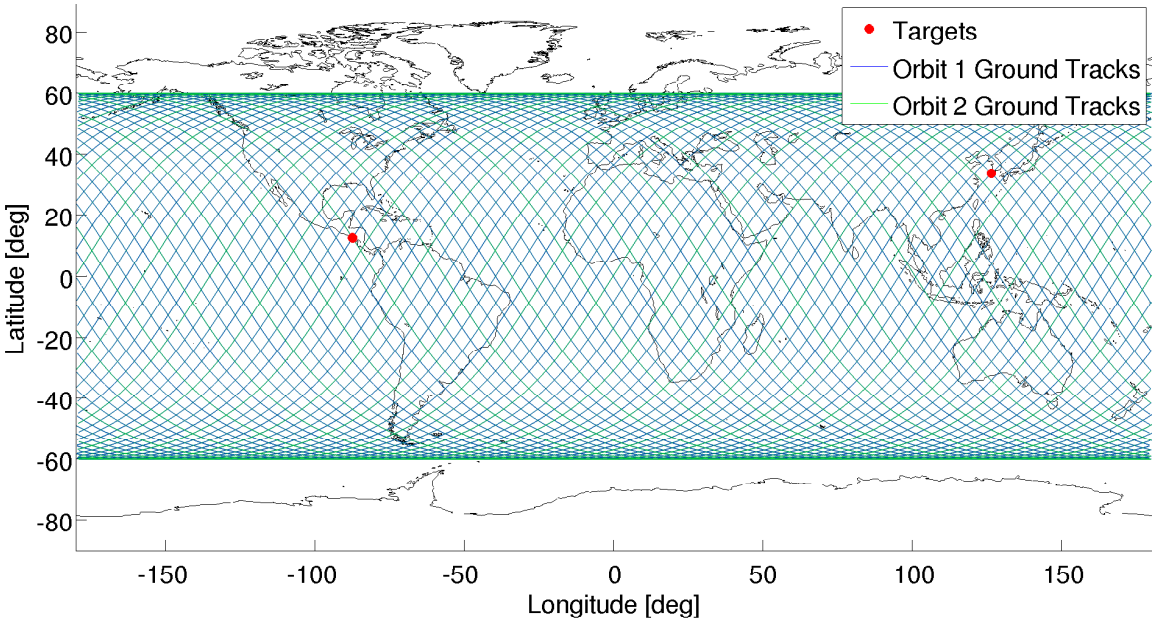


**Figure 7. Satellite repeat ground tracks for 1 Earth rotation after manoeuvring at $t = 5.5$ days. Quality of service at targeted locations is now increased due to clustering of ground tracks over target.**

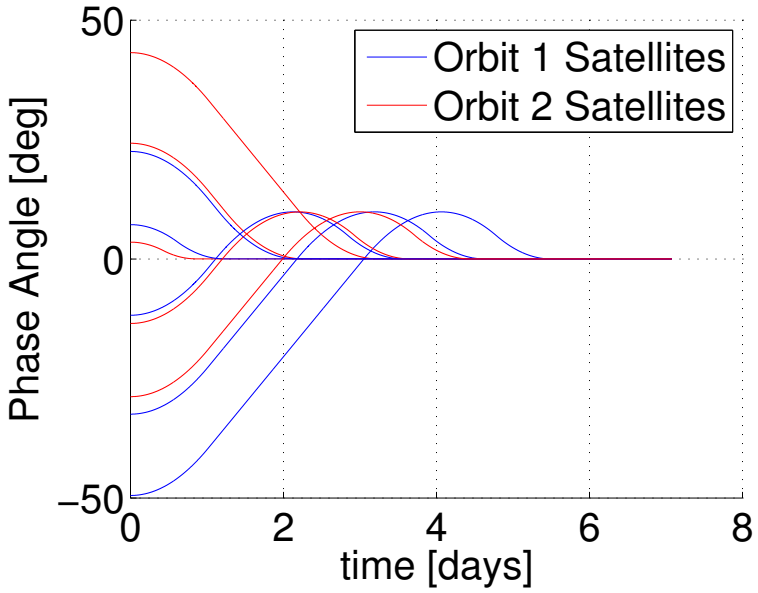


**Figure 8. Time histories of satellite phase angles.**

## CONCLUSIONS AND FUTURE WORK

This paper has demonastrated a novel method of enabling a self-organising micro-satellite constellation, capable of manipulating its repeat ground-tracks to pass over specified targets on the Earth's surface. The use of coupled selection equations allows the constellation to autonomously allocate agents to targets, and an artificial potential field controller has been designed according to Lyapunov stability theory to generate the required thrust commands.

The effectiveness of the method has been demonstrated in a mission scenario, in which two polar orbital planes containing different types of Earth imaging satellites are allocated in pairs to targets on the Earth's surface. The satellites are shown to converge upon the targets within a few days of low-thrust manoeuvring, providing the coverage necessary to meet the image resolution requirements of the mission.

Future work will focus on adapting and developing the method for other mission scenarios. In addition, the fidelity of the simulation will be increased, as orbital perturbations such as the $J_2$ effect will be included and the potential field controller will be adapted to account for these perturbations. The potential field controller will also be extended to include collision avoidane and co-location terms once for the satellites have arrived at the same orbital slot. In addition, the full dynamics will be explored, with additional control terms to counteract increases in eccentricity, etc.

## ACKNOWLEDGMENT

This work was funded by the European Research Council Advanced Investigator Grant - 227571: VISIONSPACE: Orbital Dynamics at Extremes of Spacecraft Length-Scale.

Simulation results were obtained using the EPSRC funded ARCHIE-WeSt High Performance Computer (www.archie-west.ac.uk). EPSRC grant no. EP/K000586/1.

## APPENDIX: ROTATION MATRICES

Rotation matrices used in the derivation of the analytical ground-tracks are given below:

$$R_1(\psi) = \begin{pmatrix} 1 & 0 & 0 \\ 0 & \mathrm{c}(\psi) & -\mathrm{s}(\psi) \\ 0 & \mathrm{s}(\psi) & \mathrm{c}(\psi) \end{pmatrix} \tag{41}$$

$$R_2(\psi) = \begin{pmatrix} \mathrm{c}(\psi) & 0 & \mathrm{s}(\psi) \\ 0 & 1 & 0 \\ -\mathrm{s}(\psi) & 0 & \mathrm{c}(\psi) \end{pmatrix} \tag{42}$$

$$R_3(\psi) = \begin{pmatrix} \mathrm{c}(\psi) & -\mathrm{s}(\psi) & 0 \\ \mathrm{s}(\psi) & \mathrm{c}(\psi) & 0 \\ 0 & 0 & 1 \end{pmatrix} \tag{43}$$

## REFERENCES

[1] R. Zandbergen, S. Dinwiddy, J. Hahn, E. Breeuwer, and D. Blonski, "Galileo Orbit Selection," *Proceedings of the 17th International Technical Meeting of the Satellite Division of The Institute of Navigation (ION GNSS 2004)*, Long Beach, CA, September 2004, pp. 616–623.

[2] R. A. Wiedeman and A. J. Viterbi, "The Globalstar mobile satellite system for worldwide personal communications," *3rd International Mobile Satellite Conference*, June 1993, pp. 291–296.

[3] C. Fossa, R. Raines, G. Gunsch, and M. A. Temple, "An overview of the IRIDIUM (R) low Earth orbit (LEO) satellite system," *Aerospace and Electronics Conference, 1998. NAECON 1998. Proceedings of the IEEE 1998 National*, Dayton, Ohio, July 1998, pp. 152–159.

[4] D. C. Beste, "Design of Satellite Constellations for Optimal Continuous Coverage," *Aerospace and Electronic Systems, IEEE Transactions on*, Vol. AES-14, No. 3, 1978, pp. 466–473.

[5] H. Emara and C. Leondes, "Minimum Number of Satellites for Three-Dimensional Continuous Worldwide Coverage," *Aerospace and Electronic Systems, IEEE Transactions on*, Vol. AES-13, No. 2, 1977, pp. 108–111.

[6] J. A. Atchison and M. A. Peck, "A passive, sun-pointing, millimeter-scale solar sail," *Acta Astronautica*, Vol. 67, No. 1-2, 2010, pp. 108 – 121.

[7] J. A. Atchison and M. A. Peck, "A Passive Microscale Solar Sail," *AIAA SPACE 2008 Conference and Exposition*, AIAA, September 2008.

[8] A. G. Y. Johnston and C. R. McInnes, "Autonomous Control of a Ring of Satellites," *AAS/AIAA Space Flight Mechanics Meeting*, No. AAS 97-104, Huntsville, Alabama, AAS/AIAA, AAS, February 1997.

[9] X. Duan and P. Bainum, "Low-Thrust Autonomous Control for Maintaining Formation and Constellation Orbits," *AIAA/AAS Astrodynamics Specialist Conference and Exhibit*, Providence, Rhode Island, AIAA, August 2004.

[10] X. Junhua and Z. Yulin, "A Coordination Control Method for Stationkeeping of Regressive Orbit Regional Coverage Satellite Constellation," *Proceedings of the 25th Chinese Control Conference*, Harbin, Heilongjiang, August 2006, pp. 136–139.

[11] A. Strong, *On the deployment and station keeping dynamics of N-body orbiting satellite constellations*. PhD thesis, Howard University, 2000.

[12] J. Wertz, J. Collins, S. Dawson, H. Knigsmann, and C. Potterveld, "Autonomous Constellation Maintenance," *Mission Design and Implementation of Satellite Constellations* (J. Ha, ed.), Vol. 1 of *Space Technology Proceedings*, pp. 263–273, Springer Netherlands, 1998.

[13] N. H. Shah, "Automated Station-Keeping For Satellite Constellations," Master's thesis, Massachusetts Institute of Technology, June 1997.

[14] Y. Ulybyshev, "Long-Term Formation Keeping of Satellite Constellation Using Linear-Quadratic Controller," *Journal of Guidance, Control, and Dynamics*, Vol. 21, No. 1, 1998, pp. 109–115.

[15] B. C. Gunter and D. C. Maessen, "Space-Based Distributed Computing Using a Networked Constellation of Small Satellites," *Journal of Spacecraft and Rockets*, Vol. 50, No. 5, 2013, pp. 1086–1095.

[16] B. Palmintier, C. Kitts, P. Stang, and M. Swartwou, "A Distributed Computing Architecture for Small Satellite and Multi-Spacecraft Missions," *16th Annual AIAA/USU Conference on Small Satellites*, 2002.

[17] B. C. Gunter and D. C. Maessen, "Applications of a Networked Array of Small Satellites for Planetary Observation," *AIAA/AAS Astrodynamics Specialist Conference*, Toronto, Canada, August 2010.

[18] J. Starke and M. Schanz, *Handbook of Combinatorial Optimization*, Vol. 2, ch. Dynamical System Approaches to Combinatorial Optimization, pp. 471–521. Heidelberg, New York: Springer Verlag, 2012.

[19] J. Starke, *Kombinatorische Optimierung auf der Basis gekoppelter Selektionsgleichungen*. PhD thesis, Universitet Stuttgart, Verlag Shaker, Aachen, 1997.